



Original Article

Nano-graphene oxide with antisense *walR* RNA inhibits the pathogenicity of *Enterococcus faecalis* in periapical periodontitis



Shizhou Wu ^{a,b}, Yunjie Liu ^c, Hui Zhang ^{a**}, Lei Lei ^{b*}

^a Department of Orthopedics, West China Hospital, Sichuan University, Chengdu, China

^b State Key Laboratory of Oral Diseases, Department of Preventive Dentistry, West China Hospital of Stomatology, Sichuan University, Chengdu, China

^c West China School of Public Health, Sichuan University, Chengdu, China

Received 11 June 2019; Final revision received 18 September 2019

Available online 23 October 2019

KEYWORDS

Enterococcus faecalis;
walR;
Graphene oxide;
Antisense RNA;
Periapical periodontitis

Abstract *Background/purpose:* *Enterococcus faecalis* (*E. faecalis*) is considered a predominant pathogen for persistent periapical infections. Antisense *walR* (AS*walR*) RNA was reported to inhibit the biofilm formation and sensitized *E. faecalis* to calcium hydroxide medication. The aims of this study were to investigate whether the graphene oxide (GO) nanosheets could be used to enhance antibacterial activity of AS*walR* RNA for *E. faecalis* in periapical periodontitis.

Materials and methods: We developed a graphene-based plasmid transformation system by loading antisense *walR* plasmid with GO-polyethylenimine (PEI) complexes (GO-PEI-AS*walR*). The particle size distributions and zeta-potential of the GO-PEI-AS*walR* were evaluated. Then, AS*walR* plasmids were labeled with gene encoding enhanced green fluorescent protein (AS*walR*-eGFP). The transformation efficiencies and the bacterial viability of *E. faecalis* were evaluated by confocal laser scanning microscopy. Quantitative real-time PCR assays were used to investigate the expressions of *E. faecalis* virulent genes after transformed by GO-PEI-AS*walR*. Also, the antibacterial properties of the GO-PEI-AS*walR* were validated in the rat periapical periodontitis model.

Results: We showed that GO-PEI could efficiently deliver the AS*walR* plasmid into *E. faecalis* cell. GO-PEI-AS*walR* significantly reduced virulent-associated gene expressions. Furthermore, GO-PEI-AS*walR* suppressed biofilm aggregation and improved bactericidal effects

* Corresponding author. State Key Laboratory of Oral Diseases, Department of Preventive Dentistry, West China Hospital of Stomatology, Sichuan University, No. 14 Renmin South Road, Chengdu City, Sichuan, 610041, China.

** Corresponding author. Department of Orthopedics, West China Hospital, Sichuan University, No. 37 Guoxue Alley, Wuhou District, Chengdu City, Sichuan, 610041, China.

E-mail addresses: caesarzh@163.com (H. Zhang), leilei@scu.edu.cn (L. Lei).

using infected canal models *in vitro*. In four-weeks periapical infective rat models, the GO-PEI-AS*walR* strains remarkably reduced the periapical lesion size.

Conclusion: Transformation efficiency and antibacterial prosperity of AS*walR* can be marked improved by GO-PEI based delivery system for *E. faecalis* infections.

© 2019 Association for Dental Sciences of the Republic of China. Publishing services by Elsevier B.V. This is an open access article under the CC BY-NC-ND license (<http://creativecommons.org/licenses/by-nc-nd/4.0/>).

Introduction

Enterococcus faecalis (*E. faecalis*), a gram-positive coccus, is considered a predominant pathogen for persistent periapical infections.^{1,2} *E. faecalis* can survive in a wide range of temperature, pH values, oxygen tension, humidity and harsh nutrient availability.³ Also, it is able to tolerate to conventional calcium hydroxide medication and alkaline challenge.^{4,5} Two-component signal transduction systems (TCSs) play a key role in bacterial adaption to environmental challenges.⁶ The more often related virulent factors of *E. faecalis* include *ace* (collagen binding protein), *epaA* (glycosyltransferase) and *gelE* (gelatinase).^{7,8} However, attempts to inactivate the *walRK* locus in *E. faecalis* were unsuccessful, indicating the WalRK TCS is essential for *E. faecalis* viability.⁹

Antisense RNAs (asRNAs) which regulatory activity is based on complementary mechanisms to and base-pairing to the mRNA, and this interaction results in blocking the translation to functional protein.¹⁰ Antisense RNAs have been applied to identify and investigate novel antibacterial targets for clinical applications.¹¹ We previously reported that antisense *walR* (AS*walR*) RNA interference reduced the transcripts of the virulent genes, alkaline stress tolerance ability and biofilm aggregation.¹² However, one of the biggest obstacles for the use of those therapeutic antisense oligonucleotides is their limited uptake by bacterial cells without a suitable and effective carrier system.¹³ A common transformation method is to conjugate an antisense RNA with a cell-penetrating peptide which can facilitate access process.^{12,14} Nevertheless, the shortcomings of these peptides included dubious biocompatibility, risk of adverse immunogenicity to animal cells and sensitivity to protease.¹⁵ Additionally, some bacteria that acquire mutations in genes encoding translocation proteins also resist the uptake of cell-penetrating peptides.¹⁶ Hence, a novel and effective vector with favorable biocompatibility for delivering antisense RNAs has been a hot area of research focus.

Graphene oxide (GO) nanosheets could be used to deliver nucleic acid efficiently when ionically bonded to cationic polymers.^{17,18} Polyethylenimine (PEI) is known as a kind of cationic polymer for gene transfer because of its strongly binding to DNA, effectively uptake by cells and helping delivered nucleic acids escape from the lysosomal pathways.¹⁹ When electrostatic interacted with GO, the cytotoxicity of GO-PEI complex is largely reduced.^{20,21} Through oxidation reaction the surface of GO obtains large quantities of functional groups,²² GO preferentially

interacts with nucleic acids on its surface. In this way, the adsorbed nucleic acids are effectively prevented from enzymatic nucleases.²³ Until recently, new generations of graphene-oxide nanocomposites which decreased bacterial adhesion to this nanomaterial surface of have increasing attention in antibacterial properties.^{24,25} The aim of this study was to develop a graphene-based plasmid transformation system using electrostatic interacted GO-PEI complexes loaded with antisense *walR* plasmid (GO-PEI-AS*walR*) and its antibacterial efficacy against *E. faecalis* was investigated. Furthermore, we validated the role of the GO-PEI-AS*walR* in the pathogenicity using a rat periapical periodontitis model. It was hypothesized that nanographene oxide loaded with antisense *walR* RNA will be a more effective strategy in treating *E. faecalis* infections in periapical periodontitis.

Materials and methods

Preparation of GO-PEI-AS*walR* and cytotoxicity evaluation

Bacterial strains and plasmids were listed in Table 1. The synthesis of GO-PEI complexes was proceeded as previously described.^{21,26} The optional concentration of GO-PEI based AS*walR* was determined by cytotoxicity measurements. We seeded 3T3 fibroblasts cell lines in 96-

Table 1 Bacterial strains and plasmids used in this study.

Strains and plasmids	Relevant characteristics/purpose	Source
Strains		
<i>E. faecalis</i>		
<i>E. faecalis</i> V583	Spec ^s	ATCC
AS <i>walR</i>	pDL278 (Spec ^r)	This study
<i>E. coli</i>		
DH5- α	General cloning and plasmid propagation	Invitrogen
Plasmids		
pDL278	(Spec ^r) Vector for recombinant generating	Novagen
pDL278AS <i>walR</i>	(Spec ^r) Vector for AS <i>walR</i> expression	
pDL278AS <i>walR</i> -eGFP	(Spec ^r) Vector for AS <i>walR</i> -eGFP expression	This study

well plates at a density of 1000 cells/well with GO-PEI-AS*walR* at a range of concentrations from 1000 µg/mL to 0 µg/mL with Dulbecco Modified Eagle Medium (DMEM; Hyclone, Logan, UT, USA) supplemented with 10% of fetal bovine serum (FBS; Hyclone). After 48 h or 72 h incubation (37 °C, 5% CO₂), the culture medium was removed. Then the cells were washed with phosphate buffer solution (PBS, pH = 7.4; Hyclone) twice and evaluated with a cell counting kit (CCK-8; Dojindo Laboratories, Kumamoto, Japan) for the cellular vitality. Ten microliters of CCK-8 was added in each well and the absorbance at 540 nm was detected using a microplate reader (ELX800, Gene, Hong Kong, China) after 2 h culture.

Particle size distribution, zeta potential and atomic force microscopy measurements

The particle size distribution and zeta-potential of the GO-PEI based AS*walR* samples were evaluated using Dynamic Light Scattering (DLS) and zeta-potential of the GO-PEI based AS*walR* samples were evaluated in triplicate by a Nano ZS Malvern Zetasizer (Malvern Instruments, Worcestershire, UK).²⁷ The prepared sample solution (50 µL/drop) was dropped at the coverslip, dried in room temperature and characterized by atomic force microscope (AFM) using SPM-9500J2 (Shimadzu, Tokyo, Japan) with the contact mode.

Bacterial culture and transformation

The *E. faecalis* standard strain V583 was used and grown in Brain Heart Infusion (BHI; Becton Dickinson, Franklin Lakes, NJ, USA) at 37 °C in a 5% CO₂ atmosphere. The bacterial culture and transformation were conducted as previously described.^{14,28}

Evaluation the morphology of biofilm cells

All the *E. faecalis* biofilms were imaged by scanning electron microscopy (SEM; FEI Company, Hillsboro, OR, USA), crystal violet (CV) assays and the confocal laser scanning microscopy (CLSM; TSP SP2, Leica, Solms, Germany) as previously described.^{29,30}

Transfection efficiency of GO-PEI-AS*walR* in vitro

Recombinant AS*walR* plasmids were labeled with gene encoding enhanced green fluorescent protein (AS*walR*-eGFP). AS*walR*-eGFP and GO-PEI-AS*walR*-eGFP strains were constructed according to the transformation procedures previously described.¹² The expression levels of eGFP were determined by CLSM and the transfection efficiency was determined by comparing the green fluorescent intensities. The expression of AS*walR*, *walR* and *walk* as well as virulent factors genes including *ace*, *epaA*, and *gelE* of all *E. faecalis* strains were examined using real-time polymerase chain reaction (RT-PCR). The primers were listed in Table 2.

Protein extraction and western blotting analysis

The expression of WalR protein in *E. faecalis* strains after planktonic growth was quantified by Western blotting analysis as previously described.¹⁴

Infection of root canal

For dentinal infections, a three-week old biofilm model was established as previously described.¹² Briefly, the root canal specimens were incubated in *E. faecalis* V583, AS*walR* strain, *E. faecalis* + GO strain, and *E. faecalis* + GO-PEI-AS*walR* strain respectively for 3 weeks.

Pulp-exposed periapical periodontitis lesions in rats

Animal experiments were approved by approved by The West China Hospital of Sichuan University Biomedical Research Ethics Committee (No. 2018039A) and all the procedures were conducted as previously described,³¹ following the guidelines for animal care and use of laboratory animals. Six-week-old female Sprague–Dawley rats (260–280 g) were anesthetized with ketamine/xylazine (100 and 5 mg/kg body weight, respectively) by intraperitoneal injection. An access opening was made on the occlusal surface of the left mandible first molars. Then, 0.1 mL of log-phased *E. faecalis* V583 and AS*walR* bacterial suspensions were inoculated into pulp chamber and covered with light-cure flowable resin. Four weeks post-

Table 2 Oligonucleotide primers used in this study.

Primers	Sequence 5'-3' (Forward/Reverse)	Resource
QRT-PCR		
<i>16s</i>	5'- AGCAACGCGAAGAACCTTAC-3'/5'- ATTTGACGTCATCCCCACCT-3'	Sangon Biotech
<i>ace</i>	5'- GGCGACTCAACGTTTGAC -3'/5'- TCCAGCCAATCGCCTAC -3'	Sangon Biotech
<i>gelE</i>	5'- GGAACAGACTGCCGGTTTAG -3'/5'- TTCTGGATTAGATGCACCCG -3'	Sangon Biotech
<i>walR</i>	5'- CATGGTCTCAAACGGGGTG -3'/5'- AATAACCAACCCACGACGA-3'	Sangon Biotech
<i>walk</i>	5'- CGCGTGATGTGAATGTCCA -3'/5'- GCTTCGTGATTGATCGTGCA -3'	Sangon Biotech
<i>epaA</i>	5'- GCCTATGATGCACCAGGAGA -3'/5'- CAACCATTCACCAGCCAAA -3'	Sangon Biotech
QRT-PCR for AS<i>walR</i>		
<i>PCR1</i>	5'-ATGGTGACTGCCAAAGATTCT-3'	First strand cDNA synthesis
<i>AS2</i>	5'- CGGCTTCTTTCGCATTGGTT -3'	QRT-PCR analysis

operation, the rats were sacrificed and the imaging of the rats was taken using the Quantum GX Micro-CT System (PerkinElmer, Waltham, MA). Rats were sedated using isoflurane (1–5%) and oxygen (2 L/min) mixture during imaging procedures. The scanning conditions were used as following: kV = 90; CT μ A = 72; 360° scan time = 8 s. We analyzed the reconstructed images with Analyze 12.0 (PerkinElmer, Waltham, MA). The values of relative periapical cavity were calculated when compared to the control groups.

Data analysis

The Bartlett's test was performed to assess the homogeneity of data variances and Shapiro–Wilk test was conducted to determine the normal distribution of data. One-way analysis of variance was used to compare the data, followed by pairwise multiple comparisons.

Results

Cytotoxicity and characterization of GO-PEI-ASwalR

After 48 h or 72 h of incubation with GO-PEI-ASwalR, the viability of 3T3 fibroblasts cells significantly decreased at concentrations of 60 μ g/mL or higher. The results showed that synthesized GO-PEI-ASwalR was not toxic until the concentration reached to 60 μ g/mL compared with the control group (Fig. 1A).

Dynamic Light Scattering (DLS) measurements indicated that the Z-average size of the GO were 280 nm. For GO-PEI and GP-PEI-ASwalR, Z-average sizes of 95 nm and 290 nm were obtained respectively indicating that the size of GO-PEI-ASwalR was slightly larger than GO (Fig. 1B). Using zeta potential measurement, the surface charge of GO showed negative values of approximately -21.7 mV. However, GO-PEI and GO-PEI-ASwalR complex demonstrated the positive surface charges of approximately 13.1 mV and 33.7 mV respectively (Fig. 1C). The AFM results revealed that GO-PEI-ASwalR nanosheets increased the roughness and height of the membranes compared to GO and GO-PEI membrane ($n = 10$, $P < 0.05$; Fig. 1D and E).

GO-PEI-ASwalR increased ASwalR transformation and significantly reduced virulent-associated gene expressions

Using CLSM, higher levels of GFP-expression were observed in samples induced with GO-PEI-ASwalR when compared with the ASwalR (Fig. 1F). Quantitatively, a 200% increase in GFP-expression transcripts in GO-PEI-ASwalR transformed strains was found when compared with that of ASwalR cells ($P < 0.05$; Fig. 1G). Quantitative RT-PCR showed expressions of ASwalR RNA in ASwalR and GO-PEI-ASwalR strains significantly increased by 2.8 and 6.5 folds respectively when compared to *E. faecalis* V583 strain ($n = 10$, $P < 0.05$; Fig. 2A). Correspondingly, the levels expressions of *walR* and *walK* mRNA were significantly decreased in ASwalR and GO-PEI-ASwalR strains ($n = 10$,

$P < 0.05$). Moreover, the expressions of *ace*, *gel* and *epaA* genes were the lowest in the GO-PEI-ASwalR strain ($n = 10$, $P < 0.05$) (Fig. 2A). Western blotting probed with anti-WalR antibody showed that the level of WalR protein was the lowest in the GO-PEI-ASwalR cells (Fig. 2B and C).

GO-PEI-ASwalR suppressed biofilm viability in infected canal and reduced periapical lesion size

SEM observation demonstrated that *E. faecalis* V583 cells were densely packed with extracellular matrix, whereas the GO, ASwalR and GO-PEI-ASwalR strains showed the reduced extracellular matrix in the biofilms interspersed among "blank" areas (Fig. 2D). Particularly, the very few small microcolonies were found to be randomly distributed in the GO-PEI-ASwalR strain biofilms compared to the other groups (Fig. 2D). By double staining of CLSM observation, we found that silencing of *walR* by GO-PEI-ASwalR as delivery system markedly decreased the biomass of the biofilms (Fig. 3A). The quantitative data showed that the proportions of viable bacteria were significantly decreased in GO, ASwalR and GO-PEI-ASwalR strains when compared to the *E. faecalis* V583 strains (Fig. 3B). The lowest percentage of live bacteria was detected in the GO-PEI-ASwalR strain to be $14.83 \pm 0.5\%$ ($n = 10$, $P < 0.05$). Crystal violet microtiter assays demonstrated that GO-PEI-ASwalR strain exhibited the lowest optical density (OD) values of biofilm biomass ($n = 10$, $P < 0.05$, Fig. 3C).

In general, colony-forming unit (CFU) counts significantly decreased in the GO, ASwalR and GO-PEI-ASwalR strains indicating antibacterial properties in root canals. Particularly, the average CFU counts in the GO-PEI-ASwalR strain were the lowest ($n = 10$, $P < 0.05$; Fig. 3D). Correspondingly, CLSM observation showed mixtures of bacterial cells inside the dentin (Fig. 4A). The lowest proportion of viable bacteria in the GO-PEI-ASwalR strain was $14.5 \pm 0.43\%$ ($n = 10$, $P < 0.05$; Fig. 4C), whereas the *E. faecalis* V583 strain exhibited the highest ratio ($n = 10$, $P < 0.05$; Fig. 4C). At 4 weeks post-operation, the GO, ASwalR and GO-PEI-ASwalR strains presented remarkably reduced periapical lesion size compared to the *E. faecalis* V583 group (Fig. 4B). The micro-computed tomography (μ CT) analysis was used to quantify the relative ratios of periapical cavity which indicated that GO-PEI-ASwalR group presented the lowest periapical lesion ratio while the largest periapical lesion size was observed in the *E. faecalis* V583 group (Fig. 4D).

Discussion

Conventional antibiotics may not be effective against all bacteria, especially those that develop resistance.^{7,32,33} Therefore, supplementary therapies heighten the natural defenses against the susceptible organisms and lessen use of antibiotics for the periapical infection management. It has been suggested that the overexpression of ASwalR reduced the transcripts of the virulent genes, inhibited extracellular polymeric substances (EPS) synthesis, and suppressed biofilm organization of *E. faecalis* which could be explored as a potential therapeutic strategy for the management of persistent root canal infections.¹² Due to the RNA instability, antisense RNAs are difficult for

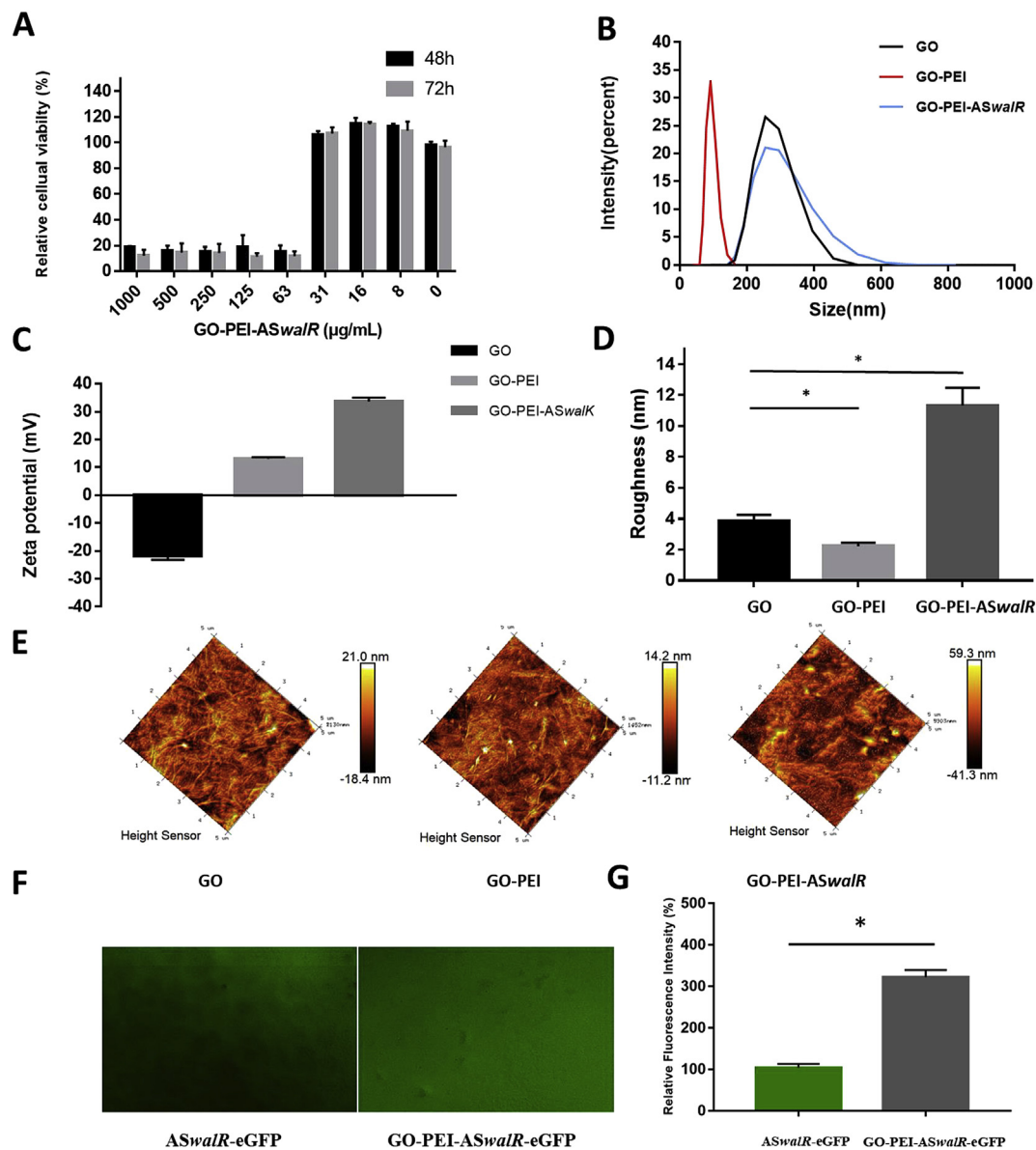


Figure 1 Cytotoxicity and characterization of GO-PEI-ASwalR. (A) The cytotoxicity of GO-PEI-ASwalR was assessed and the cell viability was determined with CCK-8 after 48 h or 72 h of incubation with GO-PEI-ASwalR (Dulbecco Modified Eagle Medium supplemented with 10% of fetal bovine serum as the blank control) (B) The particle size distributions was measured using Dynamic Light Scattering (DLS) (C) The zeta-potential of the GO-PEI based ASwalR were evaluated by a Malvern Zetasizer (D) AFM confirmed the roughness parameters of GO, GO-PEI and GO-PEI-ASwalR films ($n = 10$, $*P < 0.05$, when compared to GO control group); AFM results confirmed the roughness parameters of GO, GO-PEI and GO-PEI-ASwalR films to be 3.83 ± 0.46 nm, 2.23 ± 0.22 nm, and 9.99 ± 2.24 nm, with maximum heights of 22.40 ± 2.25 nm, 16.40 ± 3.30 nm, and 74.00 ± 20.30 nm (E) AFM images of GO, GO-PEI and GO-PEI-ASwalR complex (upper lane for 2-D view and lower lane for 3D view) (F) ASwalR plasmids were labeled with gene encoding enhanced green fluorescent protein (ASwalR-eGFP) and CLSM was applied to determine the expression level of eGFP, scale bars, $100 \mu\text{m}$ (G) The transfection efficiency was determined by comparing the green fluorescent intensities ($n = 10$, $*P < 0.05$, when compared to ASwalR-eGFP control group).

preservation, therefore we used recombinant pDL278 ASwalR overexpression plasmid for transformation. In the preliminary study, pDL278 plasmids have been transformed into *E. faecalis* as the empty vector control and did not affect the growth of *E. faecalis* cells.¹² Hence, there is a need to develop effective and stable vectors that can deliver nucleic acid molecules without detrimental effects to normal eukaryotic cells.³²

It is reported that graphene oxide (GO) can be used to deliver genes efficiently when ionically bonded to cationic polyethyleneimine (PEI) polymers.¹⁶ Therefore, we used these stable GO-PEI complexes to load antisense RNA to enhance transformation efficiency in bacteria and acquired a more efficiency than a traditional competence stimulating peptide method. These positive surface charges can favor the interaction with the negatively charged cell

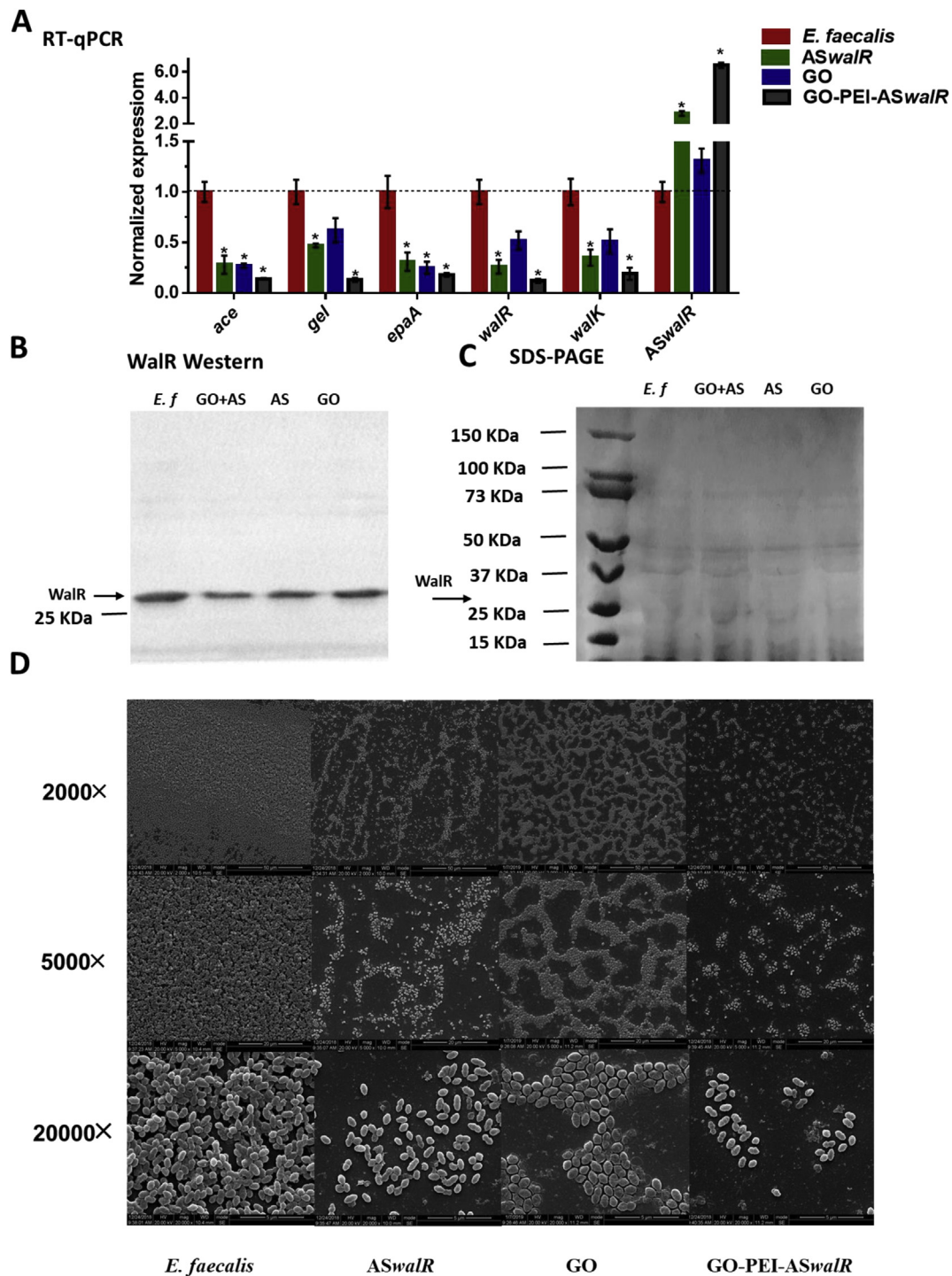


Figure 2 GO-PEI-ASwalR increased ASwalR transformation and suppressed the *E. faecalis* biofilm aggregation. (A) Quantitative RT-PCR analysis showed the gene transcripts in *E. faecalis*, ASwalR, GO and GO-PEI-ASwalR strains. *E. faecalis* gene expression was relatively quantified using 16S as an internal control and calculated based on the *E. faecalis* V583 expression, which was set as 1.0. Experiments were performed in triplicate and are presented as the mean \pm standard deviation ($n = 10$, $*P < 0.05$, when compared to *E. faecalis* V583 control group) (B) WalR production was quantified in Western blots probed with anti-WalR antibody (C) Coomassie-stained SDS-PAGE gel supporting equal loading of samples (D) SEM of *E. faecalis*, ASwalR, GO and GO-PEI-ASwalR strains. Biofilm developed in BHI for 24 h. Scale bar for 2000 magnifications, 50 μ m. Scale bars for 20000 magnifications, 5 μ m.

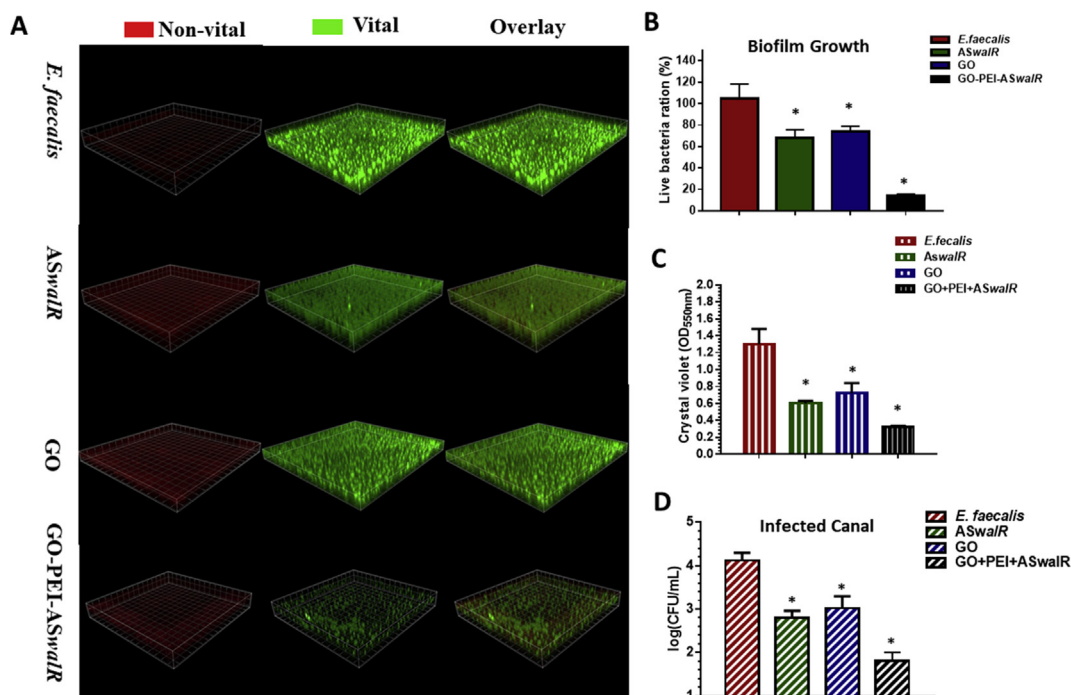


Figure 3 GO-PEI-ASwalR improved bactericidal effects in biofilm growth. (A) Double labeling of the biofilms in the *E. faecalis*, ASwalR, GO and GO-PEI-ASwalR strains. Green, viable bacteria (SYTO 9); red, dead bacteria (PI); scale bars, 100 μ m. The three-dimensional reconstruction of the biofilms was performed using Imaris 7.0.0 (B) Percentage (%) of viable *E. faecalis* cells in biofilm growth ($n = 10$, $*P < 0.05$ when compared to *E. faecalis* V583 control group; proportion of viable bacteria in the *E. faecalis* V583 was set as the 100% to estimate the live bacteria ratios) (C) Biomass was quantified by crystal violet staining ($n = 10$, $*P < 0.05$ when compared to *E. faecalis* V583 control group) (D) Number of CFUs after the *E. faecalis*, ASwalR, GO and GO-PEI-ASwalR infections [$n = 10$, $*P < 0.05$ when compared to *E. faecalis* V583 control group; log (CFU/mL)].

surface and facilitate cellular transfection.²⁶ It has been showed that the concentrations of GO-PEI lower than 50 μ g/mL had no significant effects on cell apoptosis rate.²¹ In current study, our results showed that synthesized GO-PEI-ASwalR was not toxic until the concentration reached to 60 μ g/mL (Fig. 1A). Therefore, we adopted GO-PEI-ASwalR of 30 μ g/mL as the working concentration for the subsequent studies.

The successful construction of the GO-PEI-ASwalR delivery system carrying this ASwalR was evidenced by the efficient uptake by bacterial cells and quantitative ASwalR expressions of *E. faecalis*.³⁴ To evaluate the vector transformation efficiencies, ASwalR recombinant plasmids were labeled with gene encoding enhanced green fluorescent protein (ASwalR-eGFP). The levels of GFP-expression indicated ASwalR transcripts, which revealed higher transformation efficiencies induced by GO-PEI-ASwalR when compared to pure ASwalR plasmids. Correspondingly, the quantitative RT-PCR showed expressions of ASwalR RNA in GO-PEI-ASwalR strain significantly increased by 6.5 folds compared to *E. faecalis* V583 strain (Fig. 2A). Particularly, the fold change of GO-PEI-ASwalR strain was about three times in ASwalR transformed by competence stimulating peptide indicating the GO-PEI-ASwalR probably act more efficiently than the conventional competence stimulating peptide strategy as delivery system. AFM observations revealed that the surface roughness of GO-PEI-ASwalR nanosheets increased compared to GO and GO-PEI membrane films. Due to the thicker the multilayers, the surface

parameter of material films likely increased the roughness which resulted in enhanced adhesion force.³⁵ On the other hand, altered surface charge of GO-PEI demonstrated its ability to strengthen DNA adsorption.^{17,18} Taken together, we speculated that improved delivery efficiency of the GO-PEI-ASwalR may be attributed to altered surface charge and higher surface roughness.³⁶

After 24 h biofilm establishment, the results revealed that GO-PEI-ASwalR most suppressed biofilm aggregation and reduced the cellular viability (Fig. 3A). Our previous report confirmed that ASwalR sensitized *E. faecalis* in infected canals to calcium hydroxide medication using a 3-week old biofilm model.¹² The 3-week old biofilm would be more appropriate to reflect the conditions of the biofilm during the long starvation phase because the root canal infections are likely several weeks or months old before the treatment is started.³⁷ GO sharp edge to disrupt membranes physically and GO can interfere with cellular metabolism and lead to cell necrosis/apoptosis by inducing oxidative stress. GO can form as a blanket over bacteria and isolate them from external environment, which will inhibit cells proliferation and nutrients achievement.³⁸ In the current study, the GO-PEI-ASwalR strain exhibited the lowest viable cell proportion of *E. faecalis* in dentin tubules (Fig. 4A). Moreover, the GO-PEI-ASwalR remarkably reduced periapical lesion size at 4 weeks after root canal treatment compared to the ASwalR group and the *E. faecalis* V583 group presented the large periapical lesions (Fig. 4B). In the present study, restricting the excessive in

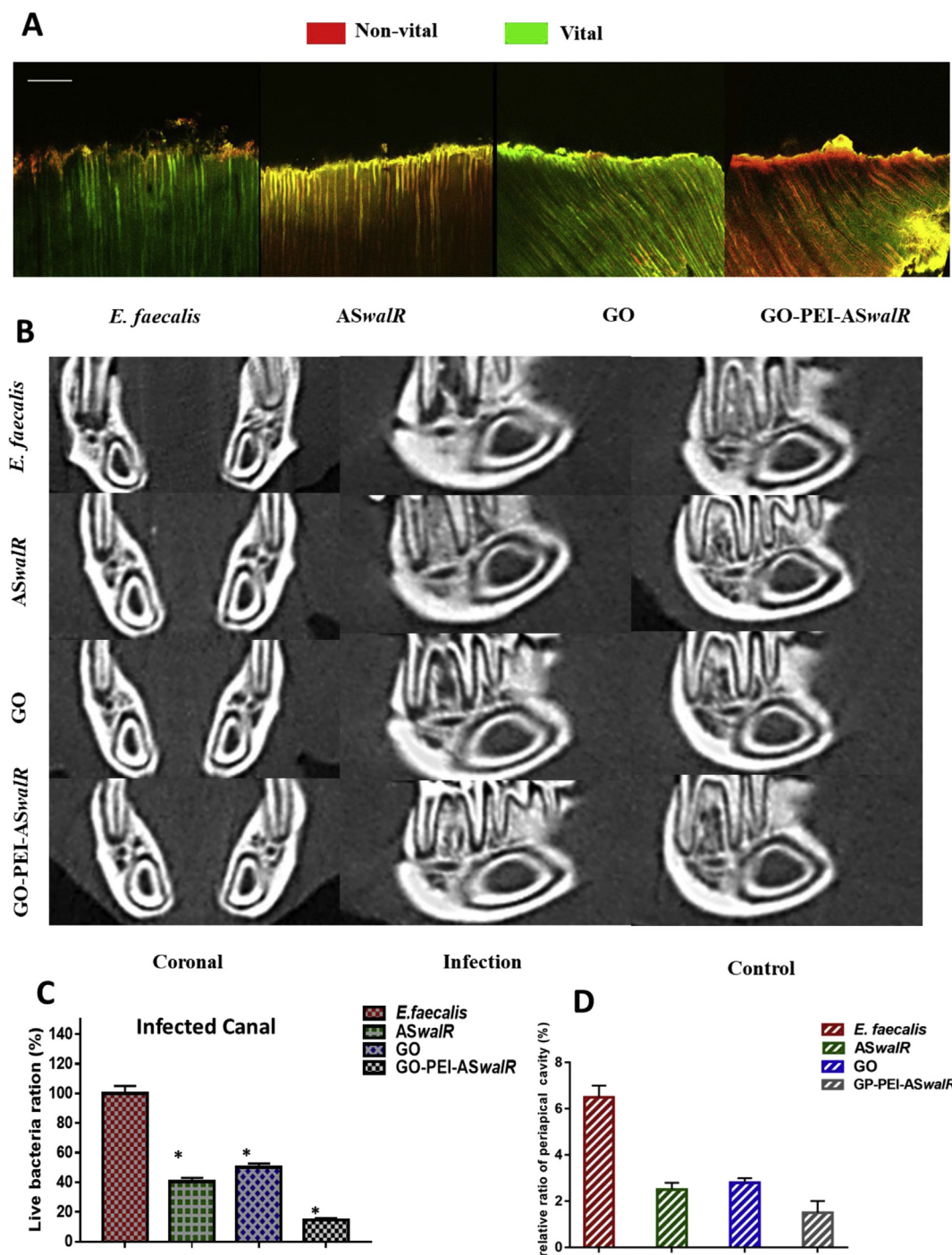


Figure 4 GO-PEI-ASwalR inhibited the bacterial viability in infected canal and reduced periapical lesion size. (A) Three-dimensional reconstruction of CLSM images of *E. faecalis* viability in dentinal tubules. Green, viable bacteria (SYTO 9); red, dead bacteria (PI), scale bars, 100 μ m (B) The reconstructed images for micro-CT scanning of the rat periapical lesions (C) Percentage (%) of viable *E. faecalis* cells in infected canal (n = 10, * P < 0.05 when compared to *E. faecalis* V583 control group; proportion of viable bacteria in the *E. faecalis* V583 was set as the 100% to estimate the live bacteria ratios) (D) The values of relative periapical cavity (%) were calculated (n = 10, * P < 0.05 when compared to *E. faecalis* V583 control group).

periapical lesions was considered an important step of the stimulating periapical repair process.³⁹ It was speculated that the pathogenicity of *E. faecalis* was markedly decreased by ASwalR interference and GO-PEI-ASwalR improved bactericidal effects in periapical periodontitis.

Graphene oxide is a kind of non-biodegradable material, which is similar to other carbon-based material. However, its biocompatibility turned out to be safer than most other types of nanomaterials, which may have an important role in its potential for clinical application.^{40,41} Future directions

needed to extend the applications of GO-PEI-AS*walR* strategy as a potential substitutive therapy for root canal infections.

In summary, we developed a graphene-based plasmid transformation system using electrostatic interacted GO-PEI complexes loaded with antisense *walR* plasmid (GO-PEI-AS*walR*). GO-PEI could efficiently deliver AS*walR* plasmid into *E. faecalis* cells with excellent transcription of AS*walR*. GO-PEI-AS*walR* significantly reduced virulent-associated gene expressions, suppressed biofilm aggregation, improved bactericidal effects in infected canal and reduced periapical lesion size. The results of present study revealed that preserving nano-graphene oxide with antisense *walR* RNA will be a more effective and stable strategy in treating *E. faecalis* infections in periapical periodontitis.

Declaration of Competing Interest

None.

Acknowledgments

This study was supported by Natural Science Foundation of China 81800964, Sichuan Provincial Natural Science Foundation of China 2018SZ0125, and Sichuan Provincial Natural Science Foundation of China 2019YFS0270, Chinese Post-doctoral Science Foundation 2018M633380.

Appendix A. Supplementary data

Supplementary data to this article can be found online at <https://doi.org/10.1016/j.jds.2019.09.006>.

References

- Gomes BP, Pinheiro ET, Gadê-Neto CR, et al. Microbiological examination of infected dental root canals. *Oral Microbiol Immunol* 2004;19:71–6.
- Pinheiro ET, Gomes BP, Ferraz CC, Sousa EL, Teixeira FB, Souza-Filho FJ. Microorganisms from canals of root-filled teeth with periapical lesions. *Int Endod J* 2003;36:1–11.
- Colomer-Winter C, Flores-Mireles AL, Baker SP, et al. Manganese acquisition is essential for virulence of *Enterococcus faecalis*. *PLoS Pathog* 2018;14:e1007102.
- Ma J, Tong Z, Ling J, Liu H, Wei X. The effects of sodium hypochlorite and chlorhexidine irrigants on the antibacterial activities of alkaline media against *Enterococcus faecalis*. *Arch Oral Biol* 2015;60:1075–81.
- Kayaoglu G, Erten H, Bodrumlu E, Ørstavik D. The resistance of collagen-associated, planktonic cells of *Enterococcus faecalis* to calcium hydroxide. *J Endod* 2009;35:46–9.
- Fukuchi K, Kasahara Y, Asai K, Kobayashi K, Moriya S, Ogasawara N. The essential two-component regulatory system encoded by *ycyF* and *ycyG* modulates expression of the *ftsAZ* operon in *Bacillus subtilis*. *Microbiol* 2000;146:1573–83.
- Dale JL, Cagnazzo J, Phan CQ, Barnes AM, Dunny GM. Multiple roles for *Enterococcus faecalis* glycosyltransferases in biofilm-associated antibiotic resistance, cell envelope integrity, and conjugative transfer. *Antimicrob Agents Chemother* 2015;59:4094–105.
- Barbosa-Ribeiro M, De-Jesus-Soares A, Zaia AA, Ferraz CC, Almeida JF, Gomes BP. Antimicrobial susceptibility and characterization of virulence genes of *Enterococcus faecalis* isolates from teeth with failure of the endodontic treatment. *J Endod* 2016;42:1022–8.
- Hancock LE, Perego M. Systematic inactivation and phenotypic characterization of two-component signal transduction systems of *Enterococcus faecalis* V583. *J Bacteriol* 2004;186:7951–8.
- Thomason MK, Storz G. Bacterial antisense RNAs: how many are there, and what are they doing? *Annu Rev Genet* 2010;44:167–88.
- Patil SD, Sharma R, Srivastava S, Navani NK, Pathania R. Downregulation of *yidC* in *Escherichia coli* by antisense RNA expression results in sensitization to antibacterial essential oils eugenol and carvacrol. *PLoS One* 2013;8:e57370.
- Wu SZ, Liu YJ, Zhang H, Lei L. The susceptibility to calcium hydroxide modulated by the essential *walR* gene reveals the role for *Enterococcus faecalis* biofilm aggregation. *J Endod* 2019;45:295–301.
- Bessa LJ, Ferreira M, Gameiro P. Evaluation of membrane fluidity of multidrug-resistant isolates of *Escherichia coli* and *Staphylococcus aureus* in presence and absence of antibiotics. *J Photochem Photobiol B* 2018;181:150–6.
- Lei L, Stipp RN, Chen T, Wu SZ, Hu T, Duncan MJ. Activity of *Streptococcus mutans* VicR is modulated by antisense RNA. *J Dent Res* 2018;97:1477–84.
- Ghosal A, Vitali A, Stach JE, Nielsen PE. Role of SbmA in the uptake of peptide nucleic acid (PNA)-peptide conjugates in *E. coli*. *ACS Chem Biol* 2013;8:360–7.
- Quijano E, Bahal R, Ricciardi A, Saltzman WM, Glazer PM. Therapeutic peptide nucleic acids: principles, limitations, and opportunities. *Yale J Biol Med* 2017;90:583–98.
- Yin D, Li Y, Lin H, et al. Functional graphene oxide as a plasmid-based Stat3 siRNA carrier inhibits mouse malignant melanoma growth in vivo. *Nanotechnology* 2013;24:105102.
- Kim H, Kim WJ. Photothermally controlled gene delivery by reduced graphene oxide-polyethylenimine nanocomposite. *Small* 2014;10:117–26.
- Putnam D, Gentry CA, Pack DW, Langer R. Polymer-based gene delivery with low cytotoxicity by a unique balance of side-chain termini. *Proc Natl Acad Sci USA* 2001;98:1200–5.
- Ding Z, Zhang Z, Ma H, Chen Y. In vitro hemocompatibility and toxic mechanism of graphene oxide on human peripheral blood T lymphocytes and serum albumin. *ACS Appl Mater Interfaces* 2014;6:19797–807.
- Dou C, Ding N, Luo F, et al. Graphene-based MicroRNA transfection blocks preosteoclast fusion to increase bone formation and vascularization. *Adv Sci* 2017;5:1700578.
- Andre Mkhoyan K, Contryman AW, Silcox J, et al. Atomic and electronic structure of graphene-oxide. *Nano Lett* 2009;9:1058–63.
- Park JS, Na HK, Min DH, Kim DE. Desorption of single-stranded nucleic acids from graphene oxide by disruption of hydrogen bonding. *Analyst* 2013;138:1745–9.
- Tang J, Chen Q, Xu L, et al. Graphene oxide-silver nanocomposite as a highly effective antibacterial agent with species-specific mechanisms. *ACS Appl Mater Interfaces* 2013;5:3867–74.
- Yousefi M, Dadashpour M, Hejazi M, et al. Anti-bacterial activity of graphene oxide as a new weapon nanomaterial to combat multidrug-resistance bacteria. *Mater Sci Eng C Mater Biol Appl* 2017;74:568–81.
- Feng L, Zhang S, Liu Z. Graphene based gene transfection. *Nanoscale* 2011;3:1252–7.
- Valencia C, Valencia CH, Zuluaga F, Valencia ME, Mina JH, Grande-Tovar CD. Synthesis and application of scaffolds of chitosan-graphene oxide by the freeze-drying method for tissue regeneration. *Molecules* 2018;23:E2651.

28. Lei L, Liu H, Cai Y, Wei X. MTAD combined with endosonic irrigation as a new approach for the disinfection of *Enterococcus faecalis* biofilm. *J Dent Sci* 2015;10:437–43.
29. Liu H, Wei X, Ling J, Wang W, Huang X. Biofilm formation capability of *Enterococcus faecalis* cells in starvation phase and its susceptibility to sodium hypochlorite. *J Endod* 2010;36:630–5.
30. Lei L, Shao M, Yang Y, Mao M, Yang Y, Hu T. Exopolysaccharide dispelled by calcium hydroxide with volatile vehicles related to bactericidal effect for root canal medication. *J Appl Oral Sci* 2016;24:487–95.
31. Shah A, Lee D, Song M, Kim S, Kang MK, Kim RH. Clastic cells are absent around the root surface in pulp-exposed periapical periodontitis lesions in mice. *Oral Dis* 2018;24:57–62.
32. Hegarty JP, Stewart Sr DB. Advances in therapeutic bacterial antisense biotechnology. *Appl Microbiol Biotechnol* 2018;102:1055–65.
33. Alekshun MN, Levy SB. Molecular mechanisms of antibacterial multidrug resistance. *Cell* 2007;128:1037–50.
34. Zhang Y, Ma W, Zhu Y, et al. Inhibiting methicillin-resistant *staphylococcus aureus* by tetrahedral DNA nanostructure-enabled antisense peptide nucleic acid delivery. *Nano Lett* 2018;18:5652–9.
35. Wong JE, Zastrow H, Jaeger W, von Klitzing R. Specific ion versus electrostatic effects on the construction of polyelectrolyte multilayers. *Langmuir* 2009;25:14061–70.
36. Gribova V, Auzely-Velty R, Picart C. Polyelectrolyte multilayer assemblies on materials surfaces: from cell adhesion to tissue engineering. *Chem Mater* 2012;24:854–69.
37. Wang Z, Shen Y, Haapasalo M. Effectiveness of endodontic disinfecting solutions against young and old *Enterococcus faecalis* biofilms in dentin canals. *J Endod* 2012;38:1376–9.
38. Palmieri V, Papi M, Conti C, Ciasca G, Maulucci G De Spirito M. The future development of bacteria fighting medical devices: the role of graphene oxide. *Expert Rev Med Devices* 2016;13:1013–9.
39. Siddiqui YD, Omori K, Ito T, et al. Resolvin D2 induces resolution of periapical inflammation and promotes healing of periapical lesions in rat periapical periodontitis. *Front Immunol* 2019;10:307.
40. Kim TH, Lee T, El-Said WA, Choi JW. Graphene-based materials for stem cell applications. *Materials* 2015;8:8674–90.
41. Shin SR, Li YC, Jang HL, et al. Graphene-based materials for tissue engineering. *Adv Drug Deliv Rev* 2016;105:255–74.